Mon. Not. R. Astron. Soc. **000**, 000–000 (0000) Printed 8 April 2014 (MN LATEX style file v2.2)

Analysis of bulk void regions

Sebastian Bustamante ⋆[1] Jaime E. Forero-Romero[2]

[1] *Instituto de Física - FCEN, Universidad de Antioquia, Calle 67 No. 53-108, Medellín, Colombia*
[2] *Departamento de Física, Universidad de los Andes, Cra. 1 No. 18A-10, Edificio Ip, Bogotá, Colombia*

8 April 2014

ABSTRACT

Key words: Cosmology: large-scale Structure of Universe, galaxies: star formation - line: formation

1 INTRODUCTION

The spatial distribution of galaxies describes a web-like pattern, the so-called cosmic web. Today it is understood that such configuration is driven by gravitational instabilities. ...

The study of the influence of the cosmic web on galaxy properties start with the seminal work of Dressler **[reference here]** and extends to recent works using large observational surveys that look for signatures of the web into the evolution of galaxy populations. With the advention of more detailed observations and sophisticated computational models it is now within our reach to understand what physical processes dominate.

This makes that the mass assembly history of a galaxy is deeply connected with its position in the cosmic web. There is an extensive body of literature on the effects of the web environment on the observable properties of galaxies.

This environmental study is also of paramount importance to understand the formation of our Galaxy. In our local neighborhood, the observations of dwarf galaxies around the Milky Way (MW) and the Andromeda galaxy (M31) show filamentary and disk-like patterns that can be linked to a preferential infall direction, very likely connected with the cosmic web where the Local Group (LG) of galaxies is embedded.

In this paper we quantify the velocity shear environment of DM halo pairs representative of the principal members of the Local Group (LG), the Milky Way (MW) and Andromeda galaxy (M31). We perform this study in an unconstrained cosmological simulation from random phases in the initial conditions, and unlike previous works, where were used constrained cosmological simulations which have been setup as to reproduce the large scale structure of the local universe, we use directly observational measurements of the kinematics properties of the local group **[Reference here]** in order to build faithful samples of LG-like systems.

We pay special attention to the correlation of the present velocity shear environment with the assembly and the kinematics properties of the pairs. The motivation to have that focus is that it has been previously shown that the LG present in three different realizations of the constrained simulations have assembly histories biased towards early formation times and absence of major mergers (ratio 1:10) in the last 10 Gyr. In the case of the kinematic properties, recent observational constrains to the galactocentric tangential velocity of M31 has enabled to establish how typical is the LG in a cosmological context **[reference to Forero-Romero et.al 2013-1]**, that is why we focus here how a specific kind of host environment biases these kinematics properties.

2 THE SIMULATION

As it was previously mentioned, we use an unconstrained cosmological simulation, the Bolshoi simulation, to identify the possible large scale environment of the Local Group. This is a similar approach to the one already used by **[reference here]**.

The Bolshoi simulation follows the non-linear evolution of a dark matter density field on a cubic volume of size $250h^{-1}$Mpc sampled with 2048^3 particles. The cosmological parameters in the simulation are $\Omega_\mathrm{m} = 0.27$, $\Omega_\Lambda = 0.73$, $h = 0.70$, $n = 0.95$ and $\sigma_8 = 0.82$ for the matter density, cosmological constant, dimensionless Hubble parameter, spectral index of primordial density perturbations and normalization for the power spectrum. The mass of each particle in the simulation is $m_\mathrm{p} = 1.4 \times 10^8 h^{-1}\mathrm{M}_\odot$.

2.1 Halos and Merger Trees

We identify halos with two algorithms, the Friends-of-Friends **[reference here]** algorithm and the Bound Density Maximum algorithm. The constructed catalogues also provide the basis for the mass aggregation history studies. We also include in the catalogues information about the substructure.

⋆ sbustama@pegasus.udea.edu.co

All the results presented here must be interpreted in term of host halos, without any information of the substructure. In particular the merger of two FOF halos corresponds to the epoch of first overlap, and not to the fusion and/or disruption of an accreted sub-halo with a dominant halo.

The linking length is $b = 0.17$ times the mean inter-particle separation. All objects with 20 particles or more are considered a bona fide halo and are included in the construction of the merger tree, this corresponds to a minimum halo mass of $M_{\rm min} = 2.70 \times 10^9 h^{-1}M_\odot$in the Bolshoi simulation.

The halo identification for the simulation was done for XX snapshots in the redshift range $0 < z < 7$ more or less evenly spaced in look-back time.

3 ALGORITHMS TO QUANTIFY THE COSMIC WEB

3.1 The tidal web (T-web)

The first algorithm we use to identify the cosmic web is based upon the diagonalization of the tidal tensor, defined as the Hessian of a normalized gravitational potential

$$T_{\alpha\beta} = \frac{\partial^2 \phi}{\partial x_\alpha \partial x_\beta} \tag{1}$$

where the physical gravitational potential has been rescaled by a factor $4\pi G\bar{\rho}$ in such a way that ϕ satisfies the following equation

$$\nabla^2 \phi = \delta, \tag{2}$$

where $\bar{\rho}$ is the average density in the Universe, G is the gravitational constant and δ is the dimensionless matter overdensity.

3.2 The velocity web (V-web)

We also use a kinematical method to define the cosmic-web environment in the simulation. The method has been thoroughly described in XXX and applied to study the shape and spin alignment in the Bolshoi simulation here XX. We refer the reader to these papers to find a detailed description of the algorithm, its limitations and capabilities. Here we summarize the most relevant points for the discussion.

The V-web method for environment finding is based on the local shear tensor calculated from the smoothed DM velocity field in the simulation. The central quantity is the following dimensionless quantity

$$\Sigma_{\alpha\beta} = -\frac{1}{2H_0}\left(\frac{\partial v_\alpha}{\partial x_\beta} + \frac{\partial v_\beta}{\partial x_\alpha}\right) \tag{3}$$

where v_α and x_α represent the α component of the comoving velocity and position, respectively. $\Sigma_{\alpha\beta}$ can be represented by a 3×3 symmetric matrix with real values, that ensures that is possible to diagonalize and obtain three real eigenvalues $\lambda_1 > \lambda_2 > \lambda_3$ whose sum (the trace of $\Sigma_{\alpha\beta}$) is proportional to the divergence of the local velocity field smoothed on the physical scale $\mathcal{R}$.

The relative strength of the three eigenvalues with respect to a threshold value λ_{th} allows for the local classification of the matter distribution into four web types: voids, sheets, filaments and peaks, which correspond to regions with 3, 2, 1 or 0 eigenvalues with values larger than λ_{th}. Below we shall discuss a novel approach to define an adequate threshold value based on the visual impression of void regions, furthermore we study other possible values based on other visual features of the cosmic web.

3.3 The cosmic web in Bolshoi

Both established schemes to quantify the cosmic web depend on continuous and smooth physical quantities, as the peculiar velocity field and the density field. In order to calculate the necessary tensors, a discretization of the simulation volume is performed, so all the properties are reduced to single values associated to discrete cells. According to this, we divide the overall volume into $(256)^3$ cells, so each cell has an associated comoving cubic volume of 0.98 Mpc h^{-1}. Finally, in order to reduce possible effects due to the discretization process, a gaussian softening is performed between neighbour cells.

Once defined the numerical details about the classification schemes, we shall analyse the dependence on the threshold value λ_{th} for each one. In Figure 1 we show the variation of the mean density parameter δ with the threshold value for cells marked as one of the two more dominant types of environment (voids and sheets).

As was previously established by **Hoffman et al. (2012)** and as can be seen in Figure 1, the behaviour of the V-web scheme is significantly more sensible to variations of the λ_{th} value compared with the T-web scheme; nevertheless, the behaviour of the mean density parameter for voids, sheets and filaments, are qualitatively quite similar for the two schemes, increasing with the value of λ_{th}. Although we shall focus our analysis on voids because they are completely dominant in the visual impression of the cosmic web, an analogous analysis might be performed for other type of environments.

On cosmic scales, the presence of highly non-linear structures implies the existence of very vast regions with density lower than the mean cosmological value due to the mass conservation. That is why the visual impression of the cosmic web should be necessarily dominated by these under-dense regions. Keeping that in mind, our novel proposal is based upon the correct quantification of these regions, so the optimal threshold value must be chosen such that: sheet regions do not invade real void regions (in such case, the mean density parameter of sheet regions would become negative) and void regions do not invade real sheet and filament regions (in such case, the mean density parameter of void regions would increase due to the contribution of over-dense regions). Thus, the optimal value is simply where the mean density parameter of sheet regions is null. According to this, we obtain the next optimal threshold values for the T-web and the V-web respectively, $\lambda^T_{opt} = 0.326$ and $\lambda^V_{opt} = 0.188$. To verify our analysis, we show in Figure 2 the visual impression for each defined critical value, and as can be seen, the chosen values reproduce properly the expected impression according to the density field.

Our classification scheme may be thought as a refinement of the recent schemes, where the threshold value is used to taking as a free parameter, based on the classic methods, where the classification is performed based on a cut off of the density field directly [references here]. So we make use of the objectivity achieved by the analysis of the mean density, but keeping all the environmental information provided by the tensorial schemes instead of the poor description provided by the density field.

4 FINDING BULK VOIDS

Following the recent growing interest in studying galaxy formation in low-density regions, we use a method based on a FOF-like algorithm to find extended regions of voids. To achieve this, we build the input catalogue for the FOF method with the coordinate of the center of every cell marked as void according to the web classification scheme adopted, furthermore we set an adequate linking length to connect even diagonal neighbour cells.

Following the work of **Forero-Romero et al. 2008**, we also perform a percolation analysis in order to select the best threshold parameter that reduces percolation in cells, thereby accounting for physical bulk void regions. In Figure 3 we show the obtained result of our percolation analysis for both web schemes. In both cases, it can be noticed that the volume of the largest void region is minimized and the volume distribution of voids is relatively flat at $\lambda_{th} = 0.0$, what means percolation is completely reduced for this threshold value. So, in spite of the previously established λ_{th} optimal values for each scheme, we shall use $\lambda_{th} = 0.0$ just for the detection of bulk void regions. Moreover, due to the domination of the large scale visual impression by voids, it is inevitable the presence of the percolation phenomenon, so the current chosen threshold value for percolation is justified because though voids are necessarily connected among them, we are just interested in detecting bulk regions.

Next, we shall calculate the reduced inertia tensor of each void region in order to determinate their principal directions of inertia and analyse the size-shape distribution of voids.

$$\tau_{ij} = \sum_{l} \frac{x_{l,i} x_{l,j}}{R_l^2} \tag{4}$$

where l is an index associated to each cell of to the current region, i and j indexes run over each spatial direction and finally R_l is defined as $R_l^2 = x_{l,1}^2 + x_{l,2}^2 + x_{l,3}^2$, all positions are measured from the respective center of mass of the region.

The eigenvalues of the reduced inertia tensor, i.e. the principal moments of inertia, are used to quantify the shape of void regions. They are denoted as τ_1, τ_2 and τ_3 such that $\tau_1 \leqslant \tau_2 \leqslant \tau_3$. In Figure 4 we show the computed distributions for τ_1/τ_2 and τ_2/τ_3, where we rather calculate histograms for these ratio quantities instead of each single value in order to avoid using an arbitrary normalization. For both schemes, it can be noticed that the shape-distribution is completely spread out, thereby indicating a non-preferred geometry of void regions, which is in agreement with the well established highly anisotropy of matter flows associated to this type of region [reference here]. Because of that, we shall look for possible alignments between the plane of rotation of halo pairs and the principal directions of inertia of the nearest void regions.

5 STATISTICS OF VOIDS AND INFLUENCE OVER DARK MATTER HALOS

6 CONCLUSIONS

ACKNOWLEDGMENTS

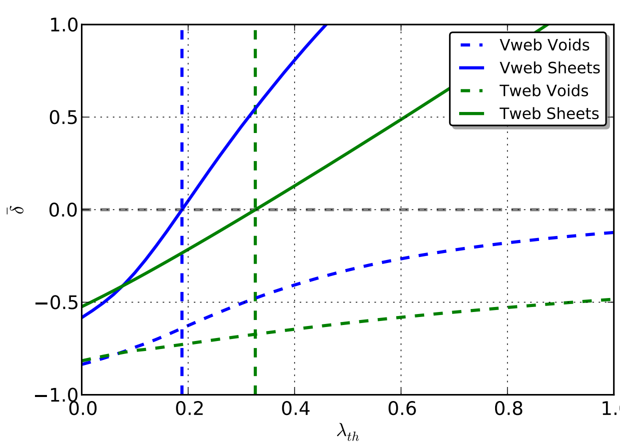

Figure 1. Mean density parameter for each one of the defined environments according to the chosen λ_{th} value and for both classification schemes. Tweb (green lines) and Vweb (blue lines). The mean density parameter is calculated by averaging all the values of the cells determined as a certain type of environment according to its eigenvalues. The optimal parameters found are $\lambda^T_{opt} = 0.326$ and $\lambda^V_{opt} = 0.188$.

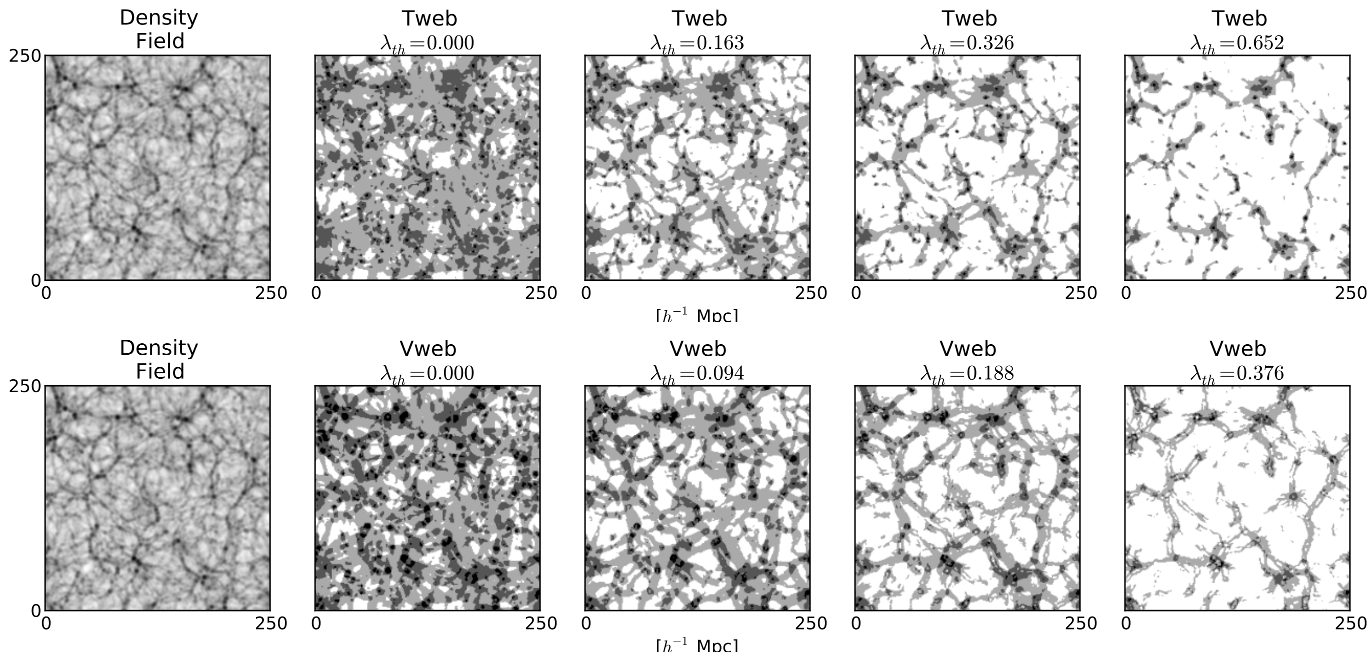

Figure 2. Visual impression of the density field (left panels), and of each classification scheme with the λ_{th} values obtained by our criteria (others panels). Our color convention for each environment is (white) - void, (light gray) - sheet, (gray) - filament, (black) - knot. For each web scheme, it has been used the previously established optimal threshold as a reference value, so plots are done with the next values $\lambda_{th} = 0.0$, $\lambda_{th} = \lambda_{opt}/2$, $\lambda_{th} = \lambda_{opt}$ and $\lambda_{th} = 2\lambda_{opt}$.

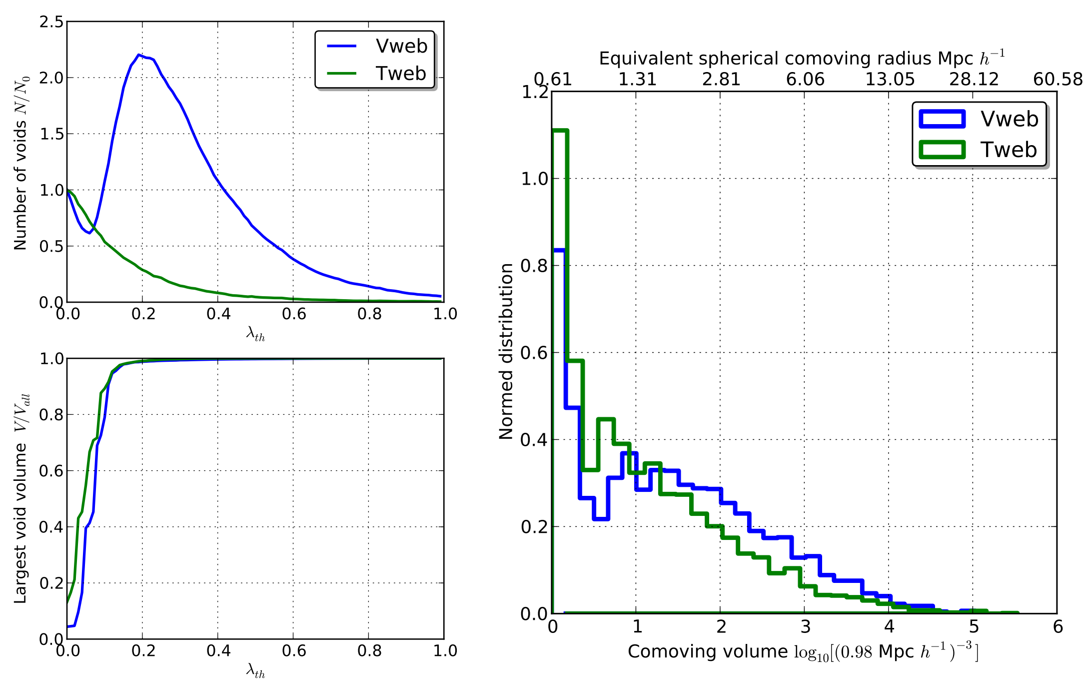

Figure 3. Percolation analysis of void regions for different λ_{th} values and for both defined classification schemes. T-web (blue lines) and V-web (green lines). Plot of the largest volume and the number of voids detected according to the threshold value λ_{th} (left panels). Size distribution histogram of void cells using the threshold value $\lambda_{th} = 0.0$ for both schemes (right panel).

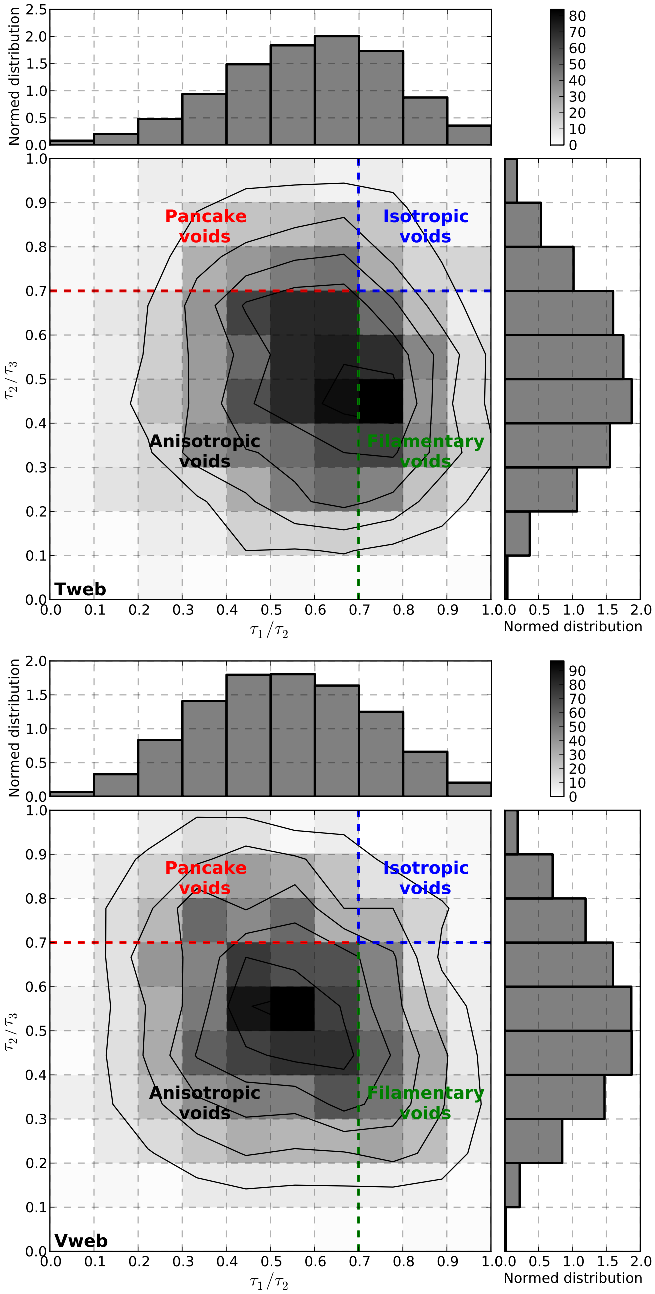

Figure 4. Histogram of eigenvalue ratio τ_1/τ_2 vs τ_2/τ_3 for the inertia tensor of void regions. T-web (upper panel) and V-web (lower panel). Number of cells per region in 2D histograms are indicated by the respective colour bar. Upper (τ_1/τ_2) and right (τ_2/τ_3) panels of each figure shows a normalized histogram of each ratio parameter. The adopted division for quantify the morphology of void regions is not well justified, it should be understood as a fuzzy and continuous limit, done just for illustrative purposes.